

Sol-Gel Spin Coating Synthesis of TiO₂ Nanostructure and Its Optical Characterization

Simeon Amole¹, Mojinyinola Kofoworola Awodele¹ , Oluwaseun Adedokun^{1*} , Momodu Jain², Ayodeji Oladiran Awodugba^{1,2} 

¹Department of Pure and Applied Physics, Ladoke Akintola University of Technology, Ogbomoso, Nigeria

²Department of Physics, The University of The Gambia, Brikama Campus, The Gambia

Email: *oadedokun@lautech.edu.ng, *adedokunoluwaseun2@gmail.com

How to cite this paper: Amole, S., Awodele, M.K., Adedokun, O., Jain, M. and Awodugba, A.O. (2019) Sol-Gel Spin Coating Synthesis of TiO₂ Nanostructure and Its Optical Characterization. *Journal of Materials Science and Chemical Engineering*, 7, 23-34.

<https://doi.org/10.4236/msce.2019.76003>

Received: May 23, 2019

Accepted: June 27, 2019

Published: June 30, 2019

Copyright © 2019 by author(s) and Scientific Research Publishing Inc. This work is licensed under the Creative Commons Attribution International License (CC BY 4.0).

<http://creativecommons.org/licenses/by/4.0/>



Open Access

Abstract

This work focuses on the sol-gel spin coating technique of TiO₂ nanostructure synthesis and its characterization. Though various methods have been used to fabricate TiO₂ nanostructure, much effort has not been exerted to achieve better photoresponsive and narrowly dispersed TiO₂ nanostructure using the sol-gel spin coating method. Therefore, it is imperative to realize the synthesis of TiO₂ nanostructures, and investigate their properties. In this work, TiO₂ is synthesized by sol-gel spin coating technique using titanium tetraisopropoxide, isopropanol, acetic acid and deionized water as starting materials and deposited on borosilicate glass substrates. The effects of annealing temperatures (300°C, 400°C and 500°C) on the structural and optical properties of the films were investigated by different techniques: Scanning Electron Microscopy (SEM), optical microscopy and UV-visible spectrophotometry. The optical characterization showed the direct band gap at 3.7 eV, 3.6 eV and 3.4 eV for 300°C, 400°C and 500°C, respectively, and the optical transmittance and reflectance spectra showed a greater performance at 500°C. The grain sizes obtained from SEM annealed at 300°C, 400°C and 500°C are found to be about 6.0 nm, 5.0 nm and 4.0 nm respectively. The grain size of TiO₂ nanostructure films decreased with increasing annealing temperatures. The results clearly indicated that the sol-gel spin coating synthesis of TiO₂ nanostructure and post-thermal treatment at 500°C cooled naturally at room temperature result in better photoresponsive and narrowly dispersed TiO₂ nanostructure films with higher photoresponsive and good optical properties.

Keywords

TiO₂, Sol-Gel Spin Coating, Grain Sizes, Nanostructure, Annealing Temperature

1. Introduction

TiO₂ nanostructure films fabricated by sol-gel spin coating have excellent optical properties suitable for application in solid-state photovoltaic solar cells. Optical characteristics of TiO₂ films under visible light though are very weak but they strongly depends on preparation methods. The main problem is that photoresponse under visible light is much lower than that under UV irradiation. Therefore, the development of new and optimized photoresponsive TiO₂ nanostructure for the existing optical properties exhibiting activity upon visible light with surface characteristics of improved performance, and of the high chemical and physical stability are crucial for broader scale utilization of photovoltaic systems in commercial applications.

Several methods have been used to prepare TiO₂ other metal oxide nanostructure films, including chemical vapor deposition (CVD) [1], pulsed laser deposition [2], reactive sputtering [3], chemical bath deposition (CBD) [4] [5] and sol-gel spin coating [6] [7]. The sol-gel spin coating has emerged as one of the new commercially viable nano-TiO₂ fabrication methodologies as this method produces samples with a uniform synthetic strategy needed for high-efficient UV-Vis optical response. In this work, TiO₂ is synthesized by a sol-gel spin coating technique and deposited on borosilicate glass substrates, using titanium tetraisopropoxide, isopropanol, acetic acid and deionized water as starting materials. By careful control of relative proportion of fixed precursor materials/solvent weight ratio of 1:3 and pH = 9.5 with nitric acid, in order to obtain a stable and clear sol of TiO₂ colloidal suspension in the nanometer range, which was dispersed on the surface of the thoroughly cleaned borosilicate glass substrates, and then spun at 4000 rev/min for 30 seconds under suction.

The effects of annealing (300°C, 400°C and 500°C) on the optical and structural properties of the films were investigated by different techniques: Ultra-violet visible spectrophotometry, scanning electron microscopy (SEM) and optical microscopy. The films were characterized by measuring the optical transmittance, reflectance spectra, energy band gap, porosity, refractive index, optical conductivity and extinction coefficient. The surface morphology of the films was viewed using AP200 MTI optical microscope. Jeol (Tokyo, Japan) JSM 5600 LV (low vacuum) scanning electron microscope (SEM) were used for structural characterization.

2. Theoretical Consideration

From the optical transmittance measurements, the absorption coefficient of the films, α was calculated, and the absorption coefficient is given by the Equation (1)

$$\alpha = \frac{\ln\left(\frac{1}{T}\right)}{d} \quad (1)$$

where T is transmittance and d is film thickness.

Meanwhile, refractive index n was calculated by the Equation (2)

$$n = \frac{1 + \sqrt{R}}{1 - \sqrt{R}} \quad (2)$$

where n is the refractive index and R is the reflectance of the film.

The optical band gap of the film was calculated by the following relation [4]:

$$(\alpha h\nu)^n = A(h\nu - E_g) \quad (3)$$

where E_g is the energy band gap, α is the absorption coefficient, $h\nu$ is the photon energy, A is the absorbance and n is either 2 for a direct band gap material or $\frac{1}{2}$ for indirect band gap material.

From the optical transmittance measurements, we may calculate the extinction coefficient of the films by the following relation [4],

$$k = \frac{\alpha\lambda}{4\pi} \quad (4)$$

where k is the extinction coefficient, λ is the wavelength of the thin film, and α is absorption coefficient of the film.

The optical conductivity of the film was calculated the following relation [8]:

$$\sigma = \frac{\alpha nc}{4\pi} \quad (5)$$

where σ is the optical conductivity of the nanostructure film, α is absorption coefficient of the film, n is the refractive index and c is the speed of light.

The thickness of the TiO₂ nanostructure was calculated using the gravimetric method [7],

$$d = \frac{M_A - M_B}{\rho A} \quad (6)$$

where M_A is the mass of substrate after deposition, M_B is the mass of substrate before deposition A is the area of the films and ρ is the density of the film.

The grain size of the synthesized TiO₂ nanostructure was calculated using the intercept technique [8].

$$g = 1/\frac{a}{b} \quad (7)$$

where a is the number of intersections and b is the actual length of the line. But actual length is the ratio of the measured length by the magnification.

The porosity of nanoporous TiO₂ nanostructure thin films can be calculated from the following relation in Equation (8)

$$\text{Porosity}(\%) = (1 - n^2 - 1/n_d^2 - 1) \times 100 \quad (8)$$

where n_d is refractive index of pore-free anatase ($n_d = 2.52$), and n is refractive index of porous TiO₂ thin films.

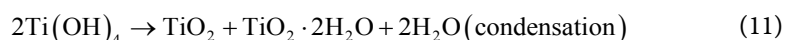
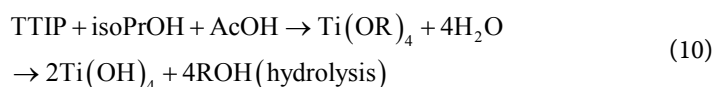
The absorbance (A), transmittance (T) and reflectance (R) satisfy the law of conservation of energy by the equation [4]:

$$A + R + T = 1 \quad (9)$$

3. Experimental Procedure

3.1. Synthesis of TiO₂ Nanostructure

At first, 15 mL of the aqueous solutions of titanium tetraisopropoxide (Ti[OCH(CH₃)₂]₄ 98+% purity, Fisher Scientific, USA) was slowly added to 30 mL of acetic acid (HCOOH 99.9% purity, Fisher Scientific, USA) in a three-neck flask, and the mixture was stirred for 5 minutes to avoid agglomeration. The mixture of deionized water (4 mL) and isopropanol (CH₃CH(OH)CH₃ 99.9%, solution BDH Ltd Poole, England) (15 mL) was added dropwise to the solution, and then stirred vigorously for another 10 minutes. After complete mixing of the solution, 4 mL of nitric acid (HNO₃) as added to the solution as stabilizer and the mixture further subjected to vigorous stirring for 20 minutes. TiO₂ colloid in the nanometer range was formed from the hydrolysis and condensation reactions of titanium alkoxide precursors. In the presence of water, titanium alkoxide hydrolyzed and subsequently polymerized to form a 3-dimensional TiO₂ network which was dispersed on the thoroughly cleaned borosilicate glass substrates, and spin at 4000 rpm for 30 seconds at room temperature. After the spin-coating step, the films were subjected to post thermal treatment at 300 °C, 400 °C and 500 °C in air for 1 hour, and then cooled at room temperature naturally.



3.2. Characterization Technique

After the preparation of the samples, different characterization techniques were used to investigate their structural and optical properties. The optical transmittance, T , and reflectance, R , of the films were measured by a UV-Vis (Lambda 950) spectrophotometer, equipped with an integrating sphere, in the wavelength range 400 - 800 nm. Porosity, optical conductivity, refractive index and extinction coefficient were calculated from the data obtained. The surface microstructure of the films was viewed using AP200 MTI optical microscope at magnification 1000 × Jeol (Tokyo, Japan) JSM 5600 LV (low vacuum) scanning electron microscope (SEM) was used to get the surface morphology of the samples.

4. Results and Discussion

4.1. Optical Studies

UV-vis transmittance spectra of TiO₂ nanostructure films for annealing temperatures at 300 °C, 400 °C and 500 °C in the wavelength range 300 - 800 nm are shown in **Figure 1**. As can be seen, all the spectrums exhibit interference fringes, which are due to the multiple reflections at the two film edges, *i.e.* at the film/air and the film/substrate interfaces. This indicates that the film surface is relatively

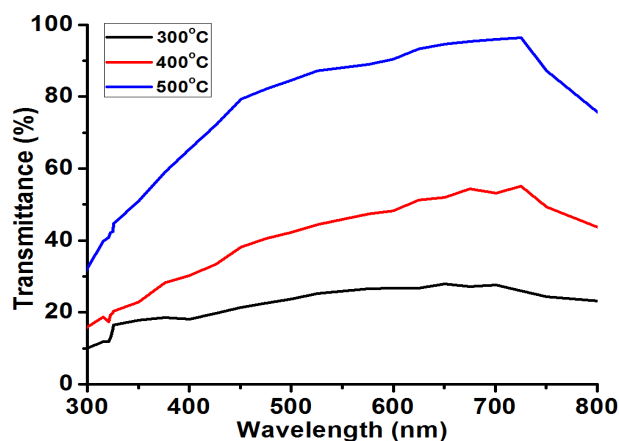


Figure 1. Transmittance-Wavelength plot of TiO₂ nanostructure annealed at 300°C, 400°C and 500°C.

smooth, uniform and exhibits a good transparency in the visible region [5] [6]. The excellent surface quality and good homogeneity of the film were confirmed from the appearance of interference fringes in the transmission spectra. The amplitude of interference spectra and the transmission percent of the TiO₂ films increase with the increase in annealing temperature. This can be due to the formation stage of anatase and with the increase in the grain size [2]. The results obtained are synonymous to the previous studies by Le *et al.* [9].

Figure 2 shows the absorption coefficient-photon energy plot for the annealed TiO₂ nanostructure films at 300°C, 400°C and 500°C temperatures range. As seen from **Figure 2**, the optical band gap was determined by extrapolating the straight-line part of the plot to the photon energy axis. From the result, it reveals that there is a gradual increase in the absorption coefficient with increasing photon energy for different annealing temperature [1] [10]. The bandgap energy of the synthesized TiO₂ nanostructure thin film decreases with the increase in annealing temperature which was found to be 3.7 eV, 3.6 eV and 3.4 eV for 300°C, 400°C and 500°C, respectively as shown in **Table 1**. This decrease was correlated with grains size decreases with temperature, and this can be linked with the formation of anatase stage [11]. These results obtained are in agreement with the previous studies by Ximello-Quebras *et al.* [12], and also near the value of 3.85 eV, found by Oh *et al.* [13] for TiO_x with a thickness of 38 nm. The decrease of the band gap cannot be due to the change of the crystallite size, since the latter decreases with the film thickness, but rather to oxygen defect band states formed in the band gap. The values of the optical band gap energy are in good agreement with those published by other authors [1] [10]. However, they are still higher than the optimum range for solar energy conversion.

Figure 3 shows the reflectance-wavelength plot of TiO₂ nanostructure annealed at 300°C, 400°C and 500°C in the wavelength range 300 - 800 nm. The reflectance is considerably high in the wavelength range of 410 - 500 nm, and a gradual fall in the reflectance in the wavelength range of 510 - 600 nm was observed. In TiO₂ nanostructure annealed at 500°C, the band gap absorption onset

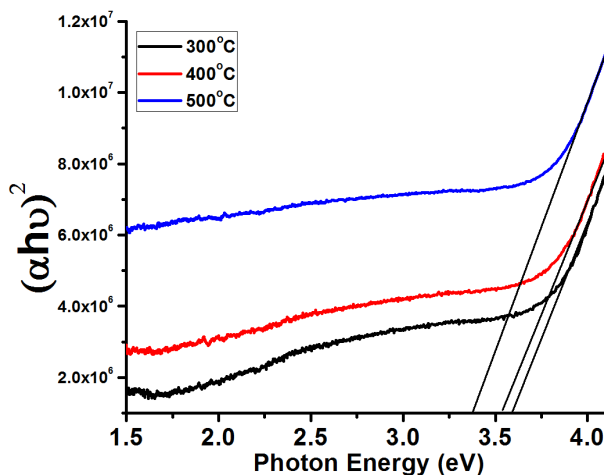


Figure 2. $(\alpha h\nu)^2$ -photon energy plot of TiO_2 nanostructure annealed at 300°C, 400°C and 500°C.

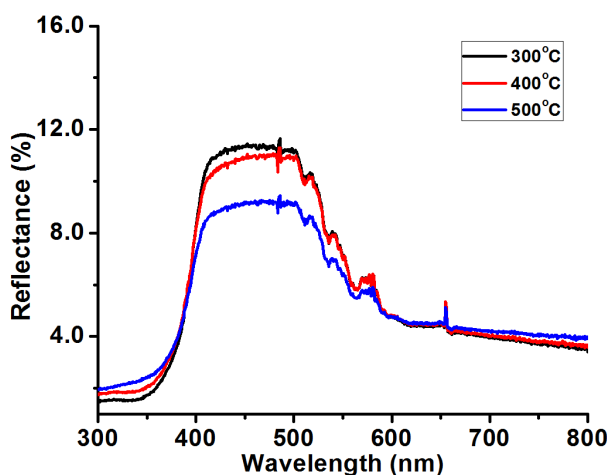


Figure 3. Reflectance-Wavelength plot of TiO_2 nanostructure annealed at 300°C, 400°C and 500°C.

Table 1. Variation of grain size, energy bandgap with different temperatures.

| Temperature (°C) | Grain size (nm) | Energy Bandgap (eV) |
|------------------|-----------------|---------------------|
| 300 | 6 | 3.7 |
| 400 | 5 | 3.6 |
| 500 | 4 | 3.4 |

shifted 420 nm from 500 nm for the TiO_2 annealed at 300°C, extending the absorption up to 420 nm, as shown in **Figure 3**. The optical absorption of TiO_2 annealed at 500°C in the visible light region was primarily located between 400 and 500 nm. TiO_2 annealed at 500°C had increased optical response compared to the case of TiO_2 nanostructure film annealed at 300°C in the visible region.

The reflectance percentage of the titanium dioxide thin film decreases with the increase in annealing temperature. This can be linked with the formation of anatase stage and with the decrease in the grain size [11].

Figure 4 shows the porosity-wavelength plot of synthesized TiO₂ nanostructure films after annealed at 300°C, 400°C, and 500°C for an hour. The result shows that the porosity of the synthesized TiO₂ nanostructure film gradually decreases with increasing wavelength, and increases with increasing temperature, which agrees with the result in other literature. The density of the TiO₂ nanostructure film increases as the porosity decreases. Higher porosity was observed at 500°C.

Figure 5 shows conductivity against photon energy plot of TiO₂ thin film for different annealing temperatures. The optical conductivity of the titanium dioxide nanostructure films increases as the temperature increases from 300°C to 500°C, and the optical responsiveness of the transparent nanostructure films were steady at a very low energy. This can be linked with the formation of anatase stage and with the decrease in the grain size [11].

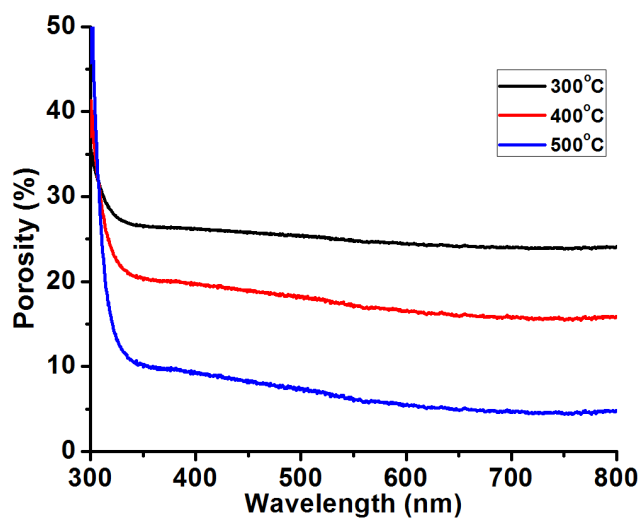


Figure 4. Porosity-wavelength plot for TiO₂ nanostructure annealed at 300°C, 400°C and 500°C.

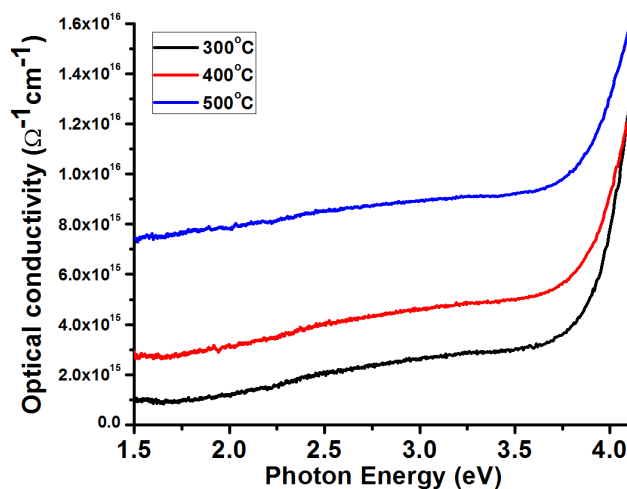


Figure 5. Optical conductivity-photon energy plot for TiO₂ nanostructure annealed at 300°C, 400°C and 500°C.

The refractive index of synthesized TiO₂ nanostructure thin films was calculated from measured UV-visible transmittance spectrum. The evaluation method used in this work is based on the analysis of UV-visible transmittance spectrum of a weakly absorbing film deposited on a non-absorbing substrate. From the result, it shows that there is a increase in the refractive index in the wavelength range 400 nm to 510 nm, and considerable attenuation is observed in the range 500 nm to 600 nm. It is noted that the refractive index and the density of nanostructure thin films of titanium oxide increases with increasing annealing temperature; due to phase transition (anatase, anatase-brookite), which increases grain sizes and/or the density of layers. The refractive index of the synthesized TiO₂ nanostructure shows better curve as the temperature increases from 300 °C to 500 °C as shown in **Figure 6**. This can be linked with the formation of anatase stage and with the decrease in the grain size [11].

The extinction coefficient of titanium dioxide thin films is shown in **Figure 7**. The extinction coefficient is high at the photon energy 4.0 eV and low at the photon energy range of 3.4 - 4.0 eV. The steady fall in the extinction coefficient may be due to the absorption of light at the grain boundary. The curve of synthesized TiO₂ nanostructure is steady at a lower extinction coefficient which agrees with the extinction coefficient of TiO₂ in other literature [1] [14]. The extinction coefficient of the titanium dioxide nanostructure films increases with the decrease in annealing temperature. This can be linked with the formation of anatase stage and with the decrease in the grain size [1] [15].

4.2. Structural Analysis

Figure 8 shows optical microscope morphology of TiO₂ nanostructures at magnification 1000×, after post thermal treatment for one hour in an oven at 300 °C, 400 °C and 500 °C, and the cooled naturally in the air. It was observed that the surface morphology of the nanostructure films show good uniformity, high homogeneity, smooth and cracks free, indicating good adhesion and regularity

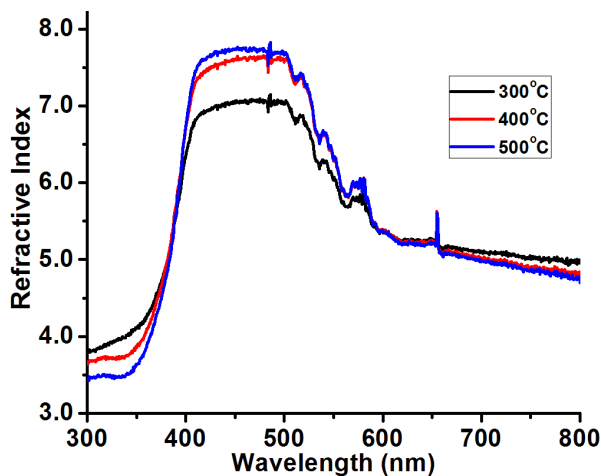


Figure 6. Refractive index-Wavelength plot of TiO₂ nanostructure annealed at 300 °C, 400 °C and 500 °C.

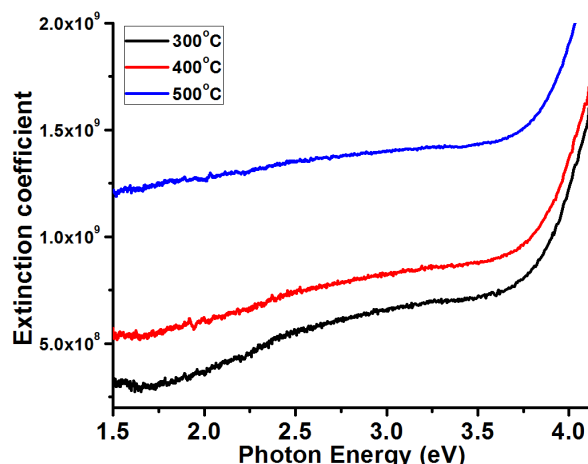


Figure 7. Extinction coefficient-photon energy plot for TiO₂ nanostructure annealed at 300°C, 400°C and 500°C.

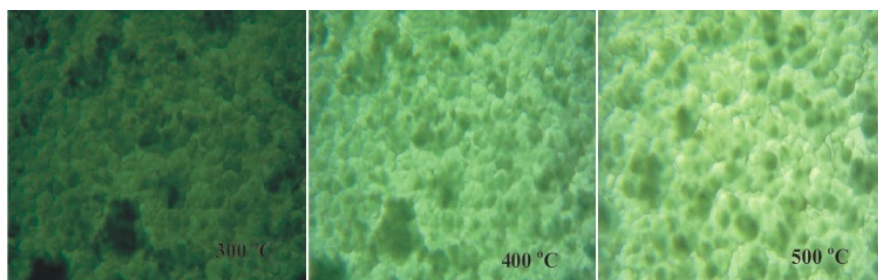


Figure 8. Optical microscope images of TiO₂ nanostructures annealed at 300°C, 400°C and 500°C.

among the layers of the prepared films.

The particles are approximately in spherical form. The bigger crystalline size was observed at 300°C. By increasing the annealing temperature from 300°C up to 500°C, it was found that the size becomes smaller and the agglomeration becomes increasingly attenuated. The effects of annealed treatment on the microstructure of the TiO₂ nanostructures were studied in a scanning electron microscope (SEM), and the obtained SEM micrographs are shown in **Figure 9**. Highly dense and well-aligned TiO₂ inter-pore structures constructed by near uniform grains of elliptical shapes were formed. It was observed that the grain size decreased with the increase in the annealing temperature. Smaller grain sizes were observed in the nanostructures at elevated temperature as shown in **Table 1**.

Grain boundaries are clearly seen in the SEM micrographs. Similar nanostructure surface has been observed by Le *et al.* [9]. At 300°C, the grain size was around 6 nm; at 400°C, the grain size decreased to 5 nm. Smaller grain sizes were observed at elevated temperature.

At 500°C, the grain size had already increased to around 4 nm. The pore density decreased in this temperature range of 300°C - 500°C, which meant better densification could be achieved. This result is consistent with what was obtained in the densification study in the literature [1] [10] [15].

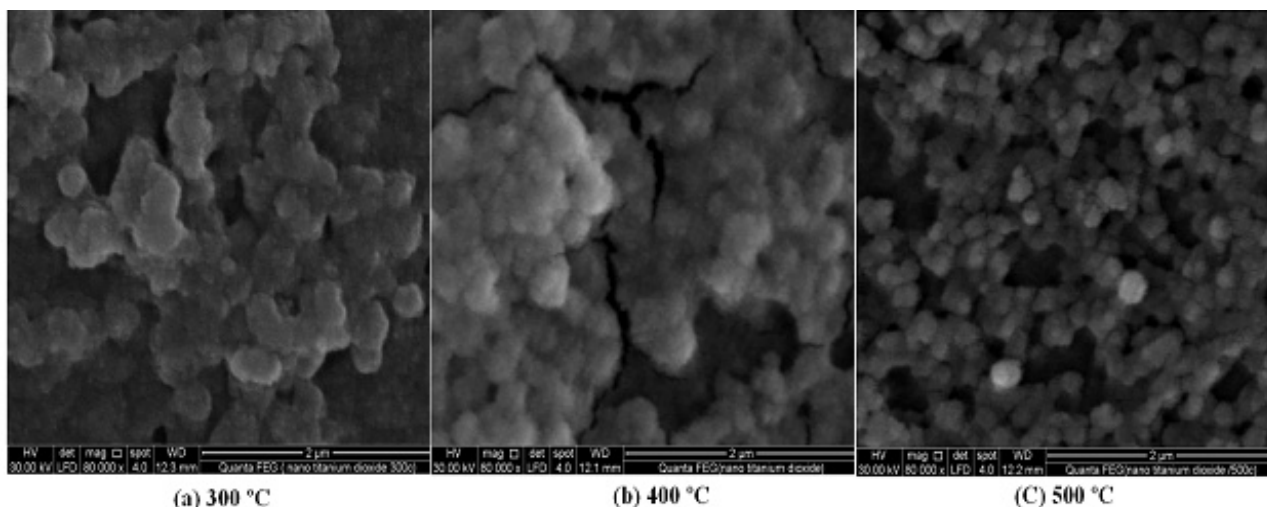


Figure 9. SEM Images of TiO₂ nanostructures annealed at 300°C, 400°C and 500°C.

5. Conclusion

TiO₂ nanostructure film has been successfully synthesized by a tandem sol-gel spin coating method. TiO₂ colloidal suspension was formed by the hydrolysis and polymerization reactions of the titanium tetraisopropoxide precursors, and dispensed on borosilicate glass substrates. The synthesized TiO₂ nanostructure films have higher transparency in the visible range (of 400 nm to 500 nm) by annealing at 500°C. The surface morphologies were observed by the SEM, and the surface morphologies showed good uniformity, and density decreases with increase in annealing temperature. The grain size decreases as temperature increases from 300°C to 500°C. At 300°C, the grain size was around 6 nm; at 400°C, the grain size increased to 5 nm. Smaller grain sizes were observed at elevated temperature. At 500°C, the grain size had already increased to around 4 nm. The bandgap energy of the synthesized TiO₂ nanostructure thin film decreased with the increase in annealing temperature which was found to be 3.7 eV, 3.6 eV and 3.4 eV for 300°C, 400°C and 500°C annealing temperatures respectively. The optical absorption, transmittance and reflectance spectra showed a greater performance at 500°C. The bandgap of TiO₂ nanostructure decreases as temperature increased. The prepared films may have a suitable application in the area of opto-electronic devices.

Acknowledgements

The authors acknowledge the efforts of the staff of Material Science and Engineering laboratory, Kwara State University, Malete, Nigeria for film deposition, SEM measurement and optical measurements.

Conflicts of Interest

The authors declare no conflicts of interest regarding the publication of this paper.

References

- [1] Yang, C., Fan, H., Xi, Y., Chen, J. and Li, Z. (2016) Effects of Depositing Temperatures on Structure and Optical Properties of TiO₂ Film Deposited by Ion Beam Assisted Electron Beam Evaporation. *Applied Surface Science*, **254**, 2685-2689. <https://doi.org/10.1016/j.apsusc.2007.10.006>
- [2] Nechache, R., Nicklaus, M., Diffalah, N., Ruediger, A. and Rosei, F. (2014) Pulsed Laser Deposition Growth of Rutile TiO₂ Nanowires on Silicon Substrates. *Applied Surface Science*, **313**, 48-52. <https://doi.org/10.1016/j.apsusc.2014.05.123>
- [3] Elen, K., Van den Rul, H., Hardy, A., Van Bael, M.K., D'Haen, J., Peeters, R., Franco, D. and Mullins J. (2009) Hydrothermal Synthesis of TiO₂ Nanorods: A Statistical Determination of the Significant Parameters in View of Reducing the Diameter. *Nanotechnology*, **20**, 55608.
- [4] Awodugba, A.O. and Adedokun, O. (2012) On the Physical and Optical Characteristics of CdS Thin Deposited by the Chemical Bath Deposition Technique. *The Pacific Journal of Science and Technology*, **12**, 334-341.
- [5] Geetha Govindasamy, Priya Murugasen and Suresh Sagadevan (2016) Investigations on the Synthesis, Optical and Electrical Properties of TiO₂ Thin Films by Chemical Bath Deposition (CBD) Method. *Material Research*, **19**, 413-419. <https://doi.org/10.1590/1980-5373-MR-2015-0411>
- [6] Singh, D., Sharma, S.D., Saini, K.K., Kant, C., Singh, N., Jain, S.C. and Sharma, C.P. (2008) Dielectric and Structural Properties of Iron Doped Titanate Nano-Composites. *IEEE International Workshop on the Physics of Semiconductor Devices (IWPSD)*, **870-871**, 20075-2689.
- [7] Bhat, J.S., Patil, A.S., Swami, N., Mulimani, B.G., Gayathri, B.R., Deshpande, N.G., Kim, G.H., Seo, M.S. and Lee, Y.P. (2010) Electron Irradiation Effects on Electrical and Optical Properties of Sol-Gel Prepared ZnO Films. *Journal Applied Physics*, **108**, Article ID: 043513. <https://doi.org/10.1063/1.3452333>
- [8] Cheng, Y.S. and Zhou, Y. (2017) Effects of Size and Shape on Filtration of TiO₂ Nanoparticles. *Aerosol Science and Technology*, **51**, 972-980. <https://doi.org/10.1080/02786826.2017.1321102>
- [9] Le, H.Q., Chua, S.J., Loh, K.P., Fitzgerald, E.A. and Koh, Y.W. (2006) Synthesis and Optical Properties of Well Aligned ZnO Nanorods on GaN by Hydrothermal Synthesis. *Nanotechnology*, **17**, 483-488. <https://doi.org/10.1088/0957-4484/17/2/023>
- [10] Sreemany, M. and Sen, S. (2004) A Simple Spectrophotometric Method for Determination of the Optical Constants and Band Gap Energy of Multiple Layer TiO₂ Thin Films. *Material Chemistry and Physics*, **83**, 169-177. <https://doi.org/10.1016/j.matchemphys.2003.09.030>
- [11] Aziz, R.A., Asyikin, N. and Sopyan, I. (2009) Synthesis of TiO₂-SiO₂ Powder Photocatalyst via Sol-Gel Method: Effect of Titanium Precursor Type on Powder Properties. *Journal of the Institution of Engineers (Malaysia)*, **70**, 34-40.
- [12] Ximello-Quiebras, J.N., Contreras-Puente, G., Aguilar-Hermández, J., Santana-Rodríguez, G. and Arias-Carbajal Readigos, A. (2014) Physical Properties of Chemical Bath Deposited CdS Thin Films. *Solar Energy Materials and Solar Cells*, **82**, 263-268. <https://doi.org/10.1016/j.solmat.2004.01.023>
- [13] Oh, H., Krantz, J., Litzov, I., Stubhan, T., Pinna, L. and Brabec, C.J. (2011) Comparison of Various Sol-Gel Derived Metal Oxide Layers for Inverted Organic Solar Cells. *Solar Energy Materials Solar Cells*, **95**, 2194-2199. <https://doi.org/10.1016/j.solmat.2011.03.023>

- [14] Viana, M.M., Soares, V.F. and Mohallem, N.D.S. (2010) Synthesis and Characterization of TiO₂ Nanoparticles. *Ceramic International*, **36**, 2047-2053. <https://doi.org/10.1016/j.ceramint.2010.04.006>
- [15] Kumar, M. and Kumar, D. (2010) The Deposition of Nano-Crystalline TiO₂ Thin Film on Silicon Using Sol-Gel Technique and Its Characterization. *Microelectronics Engineering*, **87**, 447-450. <https://doi.org/10.1016/j.mee.2009.08.025>